Dichroism in short-pulse two-color XUV plus IR multiphoton ionization of atoms

A. K. Kazansky,[1,2,3] A. V. Grigorieva,[4] and N. M. Kabachnik[2,5,6]

[1]*Departamento de Fisica de Materiales, UPV/EHU, E-20018 San Sebastian/Donostia, Spain*

[2]*Donostia International Physics Center (DIPC), E-20018 San Sebastian/Donostia, Spain*

[3]*IKERBASQUE, Basque Foundation for Science, E-48011 Bilbao, Spain*

[4]*Fock Institute of Physics, State University of Saint Petersburg, Saint Petersburg 198504, Russia*

[5]*Skobeltsyn Institute of Nuclear Physics, Lomonosov Moscow State University, Moscow 119991, Russia*

[6]*European XFEL GmbH, Albert-Einstein-Ring 19, D-22761 Hamburg, Germany*

(Received 15 March 2012; published 8 May 2012)

Circular and linear dichroism in the angular distributions of photoelectrons in multiphoton ionization of unpolarized atoms by a combination of two short pulses in the extreme ultraviolet (XUV) and infrared (IR) range is theoretically considered. A noticeable circular dichroism is predicted in the case when both XUV and IR pulses are circularly polarized. Here the dichroism may be observed not only in angle-resolved but also in angle-integrated experiments. When the XUV photons are linearly polarized while the IR pulses are circularly polarized, the circular dichroism can be observed only in angle-resolved experiments. In this case the dichroism averaged over a spectral line is small. When both pulses are linearly polarized, the photoelectron yield strongly depends on the angle between the polarizations, which leads to the considerable linear dichroism.

DOI: 10.1103/PhysRevA.85.053409 PACS number(s): 32.80.Fb, 32.80.Rm

I. INTRODUCTION

Studies of polarization effects, including different types of dichroism, constitute a substantial part of investigations of photoemission from atoms, molecules, and solids (see, for instance, Refs. [1–3]). In particular, dichroism in single-photon ionization of atoms (weak field), which is defined as the difference in the photoelectron yield for two different directions of either the polarization of the ionizing photon or of the target atom polarization, has been intensively studied in the past two decades ([4,5] and references therein). If only one electron is emitted by single-photon absorption, then the general condition for existence of the dichroism is polarization (orientation and/or alignment) of the target atom. For an unpolarized atom the dichroism is zero. (One exception is the so-called linear dichroism in the angular distribution of photoelectrons, which is nonzero also for unpolarized atoms [4]). Depending on the type of the target polarization and on the polarization of the photon beam, different kinds of dichroism are discussed: magnetic [6–8] and alignment [9,10] dichroism, circular and linear dichroism [4,11–13], and their combinations. The driving force for majority of the experimental and theoretical investigations of dichroism in atoms was the idea put forward by Klar and Kleinpoppen [14] that studies of photoionization of polarized atoms could provide sufficient measurable parameters for realization of the so-called complete experiment, i.e., experimental determination of photoionization amplitudes including their phases. Dichroism measurements facilitate extraction of those parameters from the experimental angular distributions of photoelectrons.

In many of the dichroism investigations the technique of "two-color ionization" was used [15]. Here the initial polarized state of the atom is prepared by optical pumping with an optical laser. The prepared state is subsequently ionized by an extreme ultraviolet (XUV) or x-ray photon. This technique was widely used for studying the magnetic dichroism in atomic core level photoemission [5]. Recent advance in production of intense short pulses of XUV and x-ray radiation, due to commissioning of free-electron lasers (FEL), has provided the possibility to produce another type of two-color experiments, namely to study the two-color multiphoton processes [16]. In these experiments the photoionization of atoms by XUV or x-ray photons occurs in the field of a synchronized powerful infrared (IR) laser. The emitted photoelectron, interacting with the optical field, can absorb or emit a few IR photons. Thus, in the spectrum of electrons on both sides of the photoline additional lines appear, the so-called sidebands, separated by the energy of the IR photon. The sidebands in XUV + IR two-color ionization, first studied with the sources based on high-harmonic generation [17–19], now are also investigated with the FEL radiation [20,21]. These investigations have proved to be an effective method of studying photoionization dynamics as well as to be useful instruments for characterizing the parameters of the FEL beams [20,22]. By analogy with the single-photon absorption, one can expect that the polarization analysis of the two-color multiphoton processes, including a study of dichroism, could be even more informative.

In Refs. [23,24] it was suggested to study elliptical and circular dichroism (CD) in two-color two- and three-photon ionizations of initially unpolarized atoms. This new type of dichroic measurement of the angular distribution of photoelectrons has a potential to yield the relative magnitudes and phases of the various interfering transition amplitudes. It is interesting to note that in single-color multiphoton ionization by circularly polarized light, the photoelectron yield is independent of photon helicity [25] and therefore the CD is absent. However, in two-color experiments it can exist. General analysis of the elliptical and circular dichroism in the two-photon ionization of atoms has been given in Ref. [23]. The theory was extended to the three-photon ionization in Ref. [24], where CD in the angular distribution of photoelectrons produced by linearly polarized XUV photons assisted by the circularly polarized optical laser field was investigated. In Refs. [23,24] analytical expressions for the photoelectron angular distributions in terms

of photoionization amplitudes have been given for two- and three-photon two-color ionization. However, it was noticed [24] that an extension of this method to the multiphoton case entails prohibitively cumbersome computations. Using another theoretical approach, we have predicted [26] a strong dichroic effect in multiphoton two-color ionization when both XUV and IR pulses are circularly polarized. Recently, the first experimental investigation of linear dichroism (LD) in two-color XUV + IR ionization of He atom has been performed [21]. Combining XUV radiation from the FEL in Hamburg (FLASH) with an intense synchronized optical laser, it was shown that the intensity of sidebands strongly varies as a function of relative orientation of the linear polarization vectors of the two fields. Thus, the LD in the multiple ionization of atoms, defined as the difference in photoelectron yield for parallel and perpendicular polarizations of the two beams, has been demonstrated.

In the present paper we analyze various types of dichroism in two-color XUV + IR photoionization of unpolarized atoms using the theoretical approach based on the strong-field approximation (SFA), which we developed earlier [27]. In this approach it is assumed that the IR field is moderately strong and does not affect the target atom before the XUV pulse arrives. In contrast, after ionization by the XUV pulse, the emitted electron moves in the IR field, while the influence of the ionic field is ignored. This approximation permits one to consider multiphoton ionization without limitation on the number of photons exchanged between the electron and the IR field. Some selected results have been previously published in Ref. [26]

In the next section we present the theoretical approach used for the description of the two-color multiphoton ionization. Since the model has been well documented in our recent paper [27], here we consider only basic approximations and introduce the necessary notations for the following discussion. In Sec. III different types of dichroism, circular and linear, are described and the results of their numerical simulations are presented. Section IV contains conclusions and outlook.

II. THEORETICAL DESCRIPTION OF TWO-COLOR MULTIPHOTON IONIZATION

Consider an unpolarized atom irradiated by two short (femtosecond) electromagnetic pulses, an XUV or x-ray pulse, and a pulse of a powerful IR laser. If the atom is ionized during this so-called laser-assisted photoemission (LAPE) process, in the photoelectron spectrum, apart from the usual photoline, a system of additional lines—sidebands—is observed. The sidebands appear due to absorption or emission of one or several IR photons in the process of laser-assisted XUV photoionization. Using the wave language, the origin of the sidebands can be described as the interference of the electron waves emitted at the same phase of the IR field but at different periods. The sidebands are formed if the duration of the XUV pulse is longer than the period of the IR laser light [27].

In our recent publications we have developed a theory of short-pulse LAPE, based on the numerical solution of the time-dependent Schrödinger equation (TDSE) [28–30]. In particular, we have shown that for sufficiently high kinetic energy of photoelectrons (several tens of eV and higher) and moderately strong IR fields (10^{12}–10^{13} W/cm^2) the results of the calculations agree very well with the simpler approach [31,32], which uses the SFA [33]. Since this latter approximation is simpler and less time-consuming in practical calculations than the solution of TDSE, we use it in this work.

We consider the process within the first-order time-dependent perturbation theory and use the rotating wave approximation for the XUV photon-electron interaction [34]. The amplitude of the transition from the initial state $\Psi_0 \exp(-i E_0 t)$ to the final state, which contains the ionic state $\Psi_f \exp(-i E_f t)$ and the emitted photoelectron state $\psi_{\vec{k}}$, can be written as follows (atomic units are used throughout unless otherwise indicated):

$$\mathcal{A}_{\vec{k}} = -i \int_{-\infty}^{\infty} dt\ \bar{\mathcal{E}}_X(t) \langle \Psi_f \psi_{\vec{k}}(t) \mid \hat{D} \mid \Psi_0 \rangle \exp[i(E_b - \omega_X)t], \tag{1}$$

where $\bar{\mathcal{E}}_X(t)$ is the envelope of the XUV pulse, ω_X is its mean frequency, and $E_b = E_f - E_0$ is the binding energy (positive) of the electron. The wave function $\psi_{\vec{k}}(t)$ describes the "dressed" photoelectron in the laser field, which is characterized by the final (asymptotic) momentum $\vec{k}$. The operator $\hat{D}$ is the dipole operator describing the XUV pulse interaction with atomic electrons, which can be written in the length gauge as

$$\hat{D} = \sum_i \hat{d}_i = \sum_i (\vec{\epsilon}_X \cdot \vec{r}_i), \tag{2}$$

where $\vec{\epsilon}_X$ is the polarization vector of the XUV beam, $\vec{r}_i$ are the coordinates of the ith electron, $\hat{d}_i$ is a single-electron dipole operator, and the summation is over all electrons of the atom. In the following we consider two cases, circularly and linearly polarized XUV beams. It is convenient to choose the quantization axis z along the direction of the photon beam. If the XUV photons are circularly polarized, then the dipole operator $\hat{d}$ can be expressed as

$$\hat{d}_\pm = \mp\sqrt{4\pi/3}\, r\, Y_{1,\pm1}(\hat{r}) = \sqrt{1/2}\, r(\hat{x} \pm i\hat{y}), \tag{3}$$

where $\hat{x}(\hat{y})$ is a unit vector along the $x(y)$ axis and $Y_{l,m}(\hat{r})$ is a spherical function with $\hat{r}$ being a unit radius-vector. The upper and lower signs in Eq. (3) correspond to right and left circularly polarized XUV photons, respectively. The linearly polarized beam may be presented as a superposition of right and left circularly polarized ones. Then the dipole operator can be written as

$$\hat{d}_x = \sqrt{4\pi/3}\, r\, [-Y_{1,1}(\hat{r}) + Y_{1,-1}(\hat{r})]. \tag{4}$$

Here the light is assumed to be polarized along the x axis.

Within the SFA, we ignore the influence of the laser field on the bound ionic and atomic states, which is a sufficiently good approximation for not very strong laser fields considered here. Besides, the wave function of the photoelectron is represented by the nonrelativistic Volkov wave function [35]:

$$\psi_{\vec{k}}(t) = \exp\{i[\vec{k} - \vec{A}_L(t)]\vec{r} - i\,\Phi(\vec{k},t)\}. \tag{5}$$

Here,

$$\Phi(\vec{k},t) = -\frac{1}{2}\int_t^{\infty} dt'[\vec{k} - \vec{A}_L(t')]^2, \tag{6}$$

with $\vec{A}_L(t)$ being the vector potential of the laser field, defined hereafter as $\vec{A}_L(t) = \int_t^\infty dt' \vec{\mathcal{E}}_L(t')$, where $\vec{\mathcal{E}}_L(t)$ is the IR laser electric field vector. Suppose that the IR pulse is circularly polarized, then the pulse field is:

$$\vec{\mathcal{E}}_L(t) = \frac{\bar{\mathcal{E}}_L(t)}{\sqrt{2}} [\hat{x}\cos(\omega_L t) \pm \hat{y}\sin(\omega_L t)], \tag{7}$$

where $\bar{\mathcal{E}}_L(t)$ is the envelope, ω_L is the basic frequency, and upper (lower) sign corresponds to right (left) circularly polarized IR field.

Equations (1) with (5) and (6) show that the process may be considered as photoemission of the electron at the moment t with the momentum $\vec{k}_0(t) = \vec{k} - \vec{A}_L(t)$ in the IR field, which steers the electron to the final state with the momentum $\vec{k}$ at the infinity. Here, $\vec{k}_0$ is the momentum of the electron at the moment of its emission from the atom into the IR laser field. During the propagation, the electron acquires the phase $\Phi(\vec{k},t)$. The relation of the momenta $\vec{k}$ and $\vec{k}_0(t)$ follows from the above definition. The modulus of the momenta are connected by the relation

$$k_0^2(t) = [\vec{k} - \vec{A}_L(t)]^2. \tag{8}$$

Additional relation follows from the conservation of the transverse momentum of the electron relative to the electric field. This relation depends on the direction of the IR electric field vector. For simplicity we consider the most important (from the point of view of experiments) case of collinear propagation of the XUV and IR pulses along the z axis. Then, in the chosen coordinate system, we have

$$k_0 \cos\vartheta_0 = k\cos\vartheta. \tag{9}$$

Besides

$$\exp[i\varphi_0(t)] = \frac{[k_x - A_{Lx}(t)] + i[k_y - A_{Ly}(t)]}{\left[k_0^2(t) - k_z^2\right]^{1/2}}, \tag{10}$$

where k_x (k_y) and $A_{Lx}(t)$ [$A_{Ly}(t)$] are $x(y)$ components of vectors $\vec{k}$ and $\vec{A}_L(t)$, respectively. We remind that the angles ϑ,φ are the detection angles of the electron, while ϑ_0,φ_0 are the primary angles at which the electron is ejected from the atom into the IR field. The former angles are fixed by the detection conditions, while the latter depend on the time of the emission, $\vartheta_0(t),\varphi_0(t)$.

Within the independent electron model, the matrix element in Eq. (1) can be easily reduced to the single electron matrix element $d_{\vec{k}_0} = \langle\psi_{\vec{k}}(\vec{r})|\hat{d}|\phi_{l_0}(\vec{r})\rangle$ [36], where $\phi_{l_0}(\vec{r})$ is the wave function of the electron in the initial state characterized by the orbital angular momentum l_0. Expanding the continuum electron wave function in partial waves, one can present this photoionization amplitude (for a particular projection m_0 and for circularly polarized XUV photons) as

$$d_{\vec{k}_0} = d_{l_0-1}[Y_{l_0-1,m_0\pm1}(\vartheta_0,\varphi_0) + \mathrm{Re}^{i(\delta_{l_0+1}-\delta_{l_0-1})}Y_{l_0+1,m_0\pm1}(\vartheta_0,\varphi_0)], \tag{11}$$

where $d_{l_0\pm1}$ are the partial dipole amplitudes for the transitions from the initial state with the orbital angular momentum l_0, Y_{lm} are spherical harmonics, $R = |d_{l_0+1}|/|d_{l_0-1}|$, and $\delta_{l_0\pm1}$ are the photoionization phases. If $l_0 = 0$ (ionization from s shell), only a p wave is emitted, and the amplitude is

$$d_{\vec{k}_0} = \mp d_{sp} Y_{1,\pm1}(\vartheta_0,\varphi_0). \tag{12}$$

For simplicity, in what follows we discuss s shell ionization only. A generalization to the case of $l_0 \neq 0$ is straightforward.

We are interested in the case when the sidebands consist of many lines. This happens when the optical field is comparatively strong and the energy of photoelectrons is large. The spread of the sidebands is proportional to $\sqrt{IE_p}$, where I is the intensity of the optical beam, and $E_p = \omega_X - E_b$ is the kinetic energy of the photoelectron in absence of the optical field. If the electrons are sufficiently fast (several tens of electronvolts), at moderate IR intensity the spread of the sidebands is much smaller than E_p. Since at large energies the dipole matrix element depends weakly on the energy, one can ignore its energy dependence. Then the amplitude of s shell photoionization may be approximated as

$$\mathcal{A}_{\vec{k}} \approx -i d_{sp}\, \mathcal{F}(\vec{k}), \tag{13}$$

where the function $\mathcal{F}(\vec{k})$ is defined as

$$\mathcal{F}(\vec{k}) = \mp \int_{t_0}^{t_M} dt\ \bar{\mathcal{E}}_X(t) Y_{1,\pm1}[\vartheta_0(t),\varphi_0(t)] \times \exp\left[i\int_t^\infty dt' \left(\frac{1}{2}[\vec{k} - \vec{A}(t)]^2 - E_p\right)\right], \tag{14}$$

with t_0 and t_M corresponding to the beginning and the end of the XUV pulse, respectively. The upper and lower signs correspond to the right and left circularly polarized IR radiation. Here and in the following, the XUV pulse is supposed to be shorter than the optical laser pulse, and it completely overlaps with the latter. The value $|\mathcal{F}(\vec{k})|^2$ represents the spectrum of photoelectrons in the optical laser field. In order to evaluate $\mathcal{F}(\vec{k})$ for a given set (k,ϑ,φ), one should calculate $k_0(t),\vartheta_0(t),\varphi_0(t)$ at each moment t and then integrate over t. The above simple model describes very well the peculiarity of the photoelectron spectra in two-color multiphoton ionization of atoms [27] and it is convenient for the analysis of different kinds of dichroism.

III. CIRCULAR AND LINEAR DICHROISM IN TWO-COLOR XUV + IR IONIZATION

One can consider several types of dichroism experiments with different combinations of polarization of optical laser and XUV beam. In real experiments, the polarization of FEL radiation is usually fixed, linear or (in the near future) circular. In contrast, the polarization of the optical laser can be easily manipulated to study dichroism: the circular polarization can be changed from left to right, the linear polarization can be made in two perpendicular directions. Accordingly, we consider three different cases: When the FEL beam is circularly polarized one can discuss: (a) CD in two-color ionization with circularly polarized XUV and IR beams, $\mathrm{CD}^{(\mathrm{circ})}$, i.e., the difference in electron yield for left and right circularly polarized optical beams combined with, for example, the right circularly polarized FEL beam. When the FEL beam is linearly polarized one can consider: (b) CD in two-color ionization, which is defined as the difference in the electron yield for left and right circularly polarized IR beams combined

with the linearly polarized FEL beam, $CD^{(lin)}$; and (c) LD in two-color ionization with linearly polarized XUV and IR beams, which is defined as a difference in the electron yield for two mutually perpendicular directions of optical laser linear polarization. Note that the fourth combination of the linearly polarized optical laser beam with the copropagating circularly polarized FEL beam is equivalent to the case (c), with perpendicular beam geometry. In fact, the ionization by circularly polarized FEL photons oriented and aligned the system along the beam direction; however, the angular distribution of photoelectrons after absorption of additional linearly polarized optical photons does not depend on the system orientation but only on its alignment. Therefore, this case can be reduced to the case (c) of two linearly polarized beams, perpendicular to each other.

Qualitatively, the two cases (a) and (b) are analogous to CD in single-photon absorption by oriented and aligned targets, respectively. In fact, absorption of the XUV photon creates a polarized intermediate (virtual) state, aligned if the photon is linearly polarized and oriented if it is circularly polarized. The following absorption (or emission) of the IR photons should have similar geometrical and symmetry properties as photoabsorption by the aligned or oriented target, thus revealing dichroism. Similarly, the cases (c) is analogous to LD in single-photon absorption by aligned atoms.

A. Circular IR dichroism with circularly polarized XUV pulse

Consider first the case of the two-color multiphoton ionization when both the IR and the XUV photon beams are circularly polarized. The $CD^{(circ)}$ can be measured by reversing the helicity of either of the beams. From symmetry arguments it is clear that for the case of collinear beams the resulting dichroism will be the same (with the accuracy of sign) independent of which circular polarization is reversed: of IR or XUV photons. Since the system in the initial state (unpolarized atom + photons) is axially symmetrical with respect to the beam direction (z axis) and also symmetrical with respect to reflection in the plane perpendicular to the beam direction, the angular distribution of photoelectrons should be also axially symmetrical and symmetrical with respect to the polar angle $\vartheta = \pi/2$. The considered case is analogous to the CD in the single-photon ionization from oriented targets, when the target is oriented along the beam [37]. From this analogy it follows that one can expect nonzero dichroism not only for the angle-resolved photoelectron emission but also for angle-integrated measurements.

As an example, we have calculated the spectra, the angular distribution of photoelectrons, and the $CD^{(circ)}$ for XUV + IR two-color photoionization of He. We have chosen the following parameters of the pulses: the IR pulse has a duration of 30 fs with mean wavelength of 800 nm and intensity 3.5×10^{12} W/cm^2; the XUV pulse has a duration of 2.4 fs with mean photon energy of 120 eV (circularly polarized beams with similar parameters will be soon available at FEL Fermi (Italy) [38]). The photoelectron energy is 95.4 eV. We consider the case of right circularly polarized XUV beam and right and left circularly polarized IR beam. Equations (13) and (14) are used for calculations. The dichroism is usually characterized by the ratio of the difference in the electron intensity for

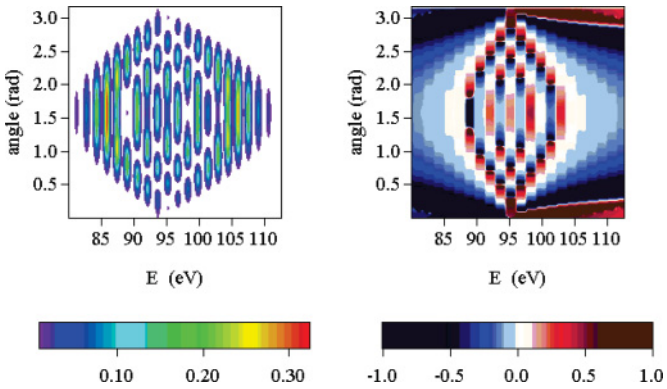

FIG. 1. (Color online) Color-scale plots of DDCS and $CD^{(circ)}$ as functions of photoelectron energy and polar emission angle ϑ. Left panel: DDCS calculated for photoionization of He by right-hand circularly polarized XUV photons at the energy of 120 eV in the field of right-hand circularly polarized IR laser (800 nm, 3.5×10^{12} W/cm^2). See other parameters in text. Right panel: Circular dichroism [Eq. (15)] calculated for the same parameters.

right and left circularly polarized beam and the sum of these intensities:

$$CD^{(circ)} = \frac{|\mathcal{A}_{\vec{k}}^{R}|^2 - |\mathcal{A}_{\vec{k}}^{L}|^2}{|\mathcal{A}_{\vec{k}}^{R}|^2 + |\mathcal{A}_{\vec{k}}^{L}|^2}, \tag{15}$$

where $\mathcal{A}_{\vec{k}}^{R}$ and $\mathcal{A}_{\vec{k}}^{L}$ are the amplitudes of the two-color photoionization with right and left circularly polarized IR photons, respectively. The results of calculations are presented in Figs. 1–4. In two-color experiments at FELs, the phase of the IR laser is usually not stabilized. Therefore, in the calculations we have simulated this effect by averaging over the time delay between IR and XUV pulses within one IR optical cycle. As it was shown in Ref. [26], the effect of averaging is not large since the dichroism is weakly dependent on the time delay between the XUV and IR pulses.

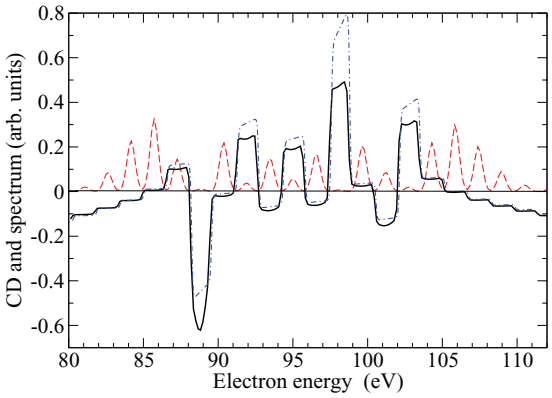

FIG. 2. (Color online) Theoretical spectrum (in arbitrary units) for laser-assisted photoionization by right circularly polarized XUV and IR light (red dashed line) and $CD^{(circ)}$ in absolute units (black solid line) at emission angle $\vartheta = \pi/2$. The results are averaged over the time delay between IR and XUV pulses within one optical period. The parameters are the same as in Fig. 1. Dot-dashed line shows the dichroism calculated for a long IR pulse using Eqs. (16)–(18).

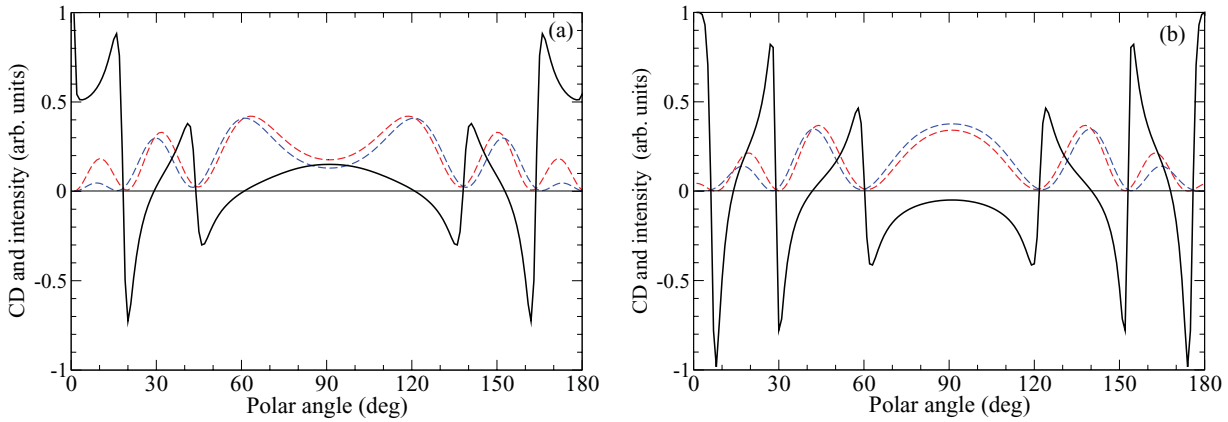

FIG. 3. (Color online) Calculated angular distributions of photoelectrons (in arbitrary units) generated by left (blue long-dashed line) and right (red short-dashed line) circularly polarized IR light and angular distribution of $CD^{(circ)}$ in absolute units (black solid line): (a) for the central line at the energy of 95.4 eV and (b) for the first sideband at the energy of 97.0 eV. The results are averaged over the time delay between IR and XUV pulses within one optical period. All parameters are the same as in Fig. 1.

In Fig. 1 we show the two-dimensional color-scale plots of the angular and energy distribution of the photoelectrons, i.e., double differential cross section (DDCS), and of the CD. In the spectra (Fig. 1, left panel) one can clearly see the system of sidebands, their number and intensity strongly vary with the emission angle. The maximal number of sidebands is at $\vartheta = \pi/2$, where the optical laser field is parallel to the emission direction. At $\vartheta = 0$ and π only the central photoelectron line is seen since the IR field, perpendicular to the electron motion, does not affect it. The right panel shows the calculated CD. For each particular angle and for low-order sidebands the CD alternates its sign from sideband to sideband. Interestingly, the CD is practically constant in every sideband; it changes abruptly between the sidebands. For higher-order sidebands the sign of CD is permanent (negative). Also, for each individual sideband of low order the CD changes its sign with the emission angle. We note that the stripes of large CD at the angles close to zero and 180° have little meaning, since the corresponding cross sections in these area are vanishingly small [see Fig. 1 (left panel)].

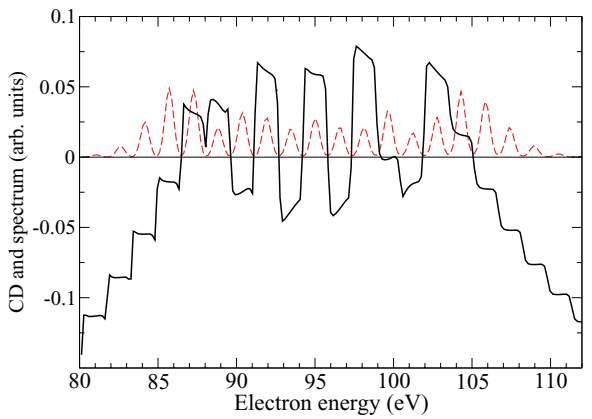

FIG. 4. (Color online) Angle-integrated cross section (red dashed curve) in arbitrary units and $CD^{(circ)}$ in absolute units (black solid curve), calculated for the same parameters as in Fig. 1. The results are averaged over the time delay between IR and XUV pulses within one optical period.

Figure 2 shows the spectrum and the dichroism for the emission angle of $\vartheta = \pi/2$ (a cut of the plots in Fig. 1). The stepwise character and the alternating sign of the CD is clearly seen. The angular distributions of photoelectrons as well as the angular distribution of the CD is presented in Fig. 3 for two particular spectral lines, at the energies 95.4 and 97.0 eV. The photoelectron angular distributions produced by left and right circularly polarized optical photons are quite similar but slightly shifted with respect to each other. This shift causes a typical dispersion-like behavior of the CD which changes sign abruptly at the angles where the angular distribution curves cross each other.

Figure 4 presents the angle-integrated spectrum and the corresponding CD. Although the general character of the CD energy dependence is the same as for particular angles, the absolute value of the dichroism is only several percent which is several times smaller than in the angle-resolved case. However, experimental observation of this small effect may be possible due to much larger statistics in angle-integrated experiments.

It is of interest to consider long XUV and IR pulses because in this case it is possible to obtain analytical result for the dichroism. As it is shown in the Appendix, when both XUV and IR pulses are right circularly polarized, the factor $\mathcal{F}(\vec{k})$, Eq. (14), can be expressed as

$$\mathcal{F}_R(\vec{k}) = \sqrt{\frac{3}{8\pi}} \sum_{n=-\infty}^{+\infty} \tilde{\mathcal{E}}_X^{(n)} i^n \exp[i(1-n)\varphi] \times \left[\sin\vartheta \left(1 - \frac{n\omega_L}{k^2}\right) J_n(q) + \frac{A_L}{k} J_{n-1}(q) \right], \quad (16)$$

where $q = kA_L \sin\vartheta/(\omega_L\sqrt{2})$, $J_n(q)$ is the Bessel function and the following notation is introduced:

$$\tilde{\mathcal{E}}_X^{(n)} = \int_{-\infty}^{\infty} dt \tilde{\mathcal{E}}_X(t) \exp\left[i \left(E_b - \omega_X + \frac{k^2}{2} + n\omega_L \right) t \right]. \quad (17)$$

For the case of left circular polarization of the IR pulse, Eq. (16) becomes

$$\mathcal{F}_L(\vec{k}) = \sqrt{\frac{3}{8\pi}} \sum_{n=-\infty}^{+\infty} \tilde{\mathcal{E}}_X^{(n)} i^n \exp[i(n+1)\varphi] \times \left[\sin\vartheta \left(1 - \frac{n\omega_L}{k^2}\right) J_n(q) + \frac{A_L}{k} J_{n+1}(q) \right]. \quad (18)$$

If the XUV pulse is sufficiently long, covering many oscillations of the IR field, then the function $\tilde{\mathcal{E}}_X^{(n)}$ is close to δ function:

$$\tilde{\mathcal{E}}_X^{(n)} \to \tilde{\mathcal{E}}_X 2\pi\delta\left(E_b - \omega_X + \frac{k^2}{2} + n\omega_L\right). \quad (19)$$

In this case for each of the sidebands (for each n) one can ignore the contributions from all other terms as well as interference between the sidebands. Then the intensity of the sideband, I_n, is proportional to the square of the nth term in the sums (16),(18): $I_n \sim |\mathcal{F}_{R(L)}^{(n)}|^2$ for right R and left L circularly polarized IR fields. Using the analytical Eqs. (16) and (18) one can calculate the $\mathrm{CD}^{(\mathrm{circ})}$ (for details see Appendix). For a particular sideband of the order n one obtains the dichroism

$$\mathrm{CD}^{(\mathrm{circ})} = 2\frac{A_L}{k} J_n(q) \frac{dJ_n(q)}{dq} \left[\sin\vartheta\left(1 - \frac{n\omega_L}{k^2}\right) + \frac{n\omega_L}{k^2 \sin\vartheta}\right] \times \left\{ J_n^2(q) \left[\sin\vartheta\left(1 - \frac{n\omega_L}{k^2}\right) + \frac{n\omega_L}{k^2\sin\vartheta}\right]^2 + \frac{A_L^2}{k^2}\left[\frac{dJ_n(q)}{dq}\right]^2 \right\}^{-1}. \quad (20)$$

In this expression the denominator (expression in curly brackets) is the sum of squares of the two terms, while the numerator is the product of these terms; thus, the values of CD are limited to the interval [-1,1] as it should be according to the definition. Moreover, since the expression in square brackets in the numerator is always positive, the zeros of the CD are determined by the zeros of Bessel functions or their derivatives. Using Eq. (20) we have calculated the CD for the same atomic parameters as above. The spectrum was simulated by a sum of Gaussian with the appropriate positions and width. The result is shown in Fig. 2 by a dot-dashed line. Comparing it with more accurate calculations (solid line) we see that the results are rather close for all lines except for a couple of weak lines. Thus Eq. (20) can be used for estimation of CD in case of comparatively long pulses.

B. Circular IR dichroism with linearly polarized XUV pulse

Now we consider the case when the ionization is produced by the linearly polarized XUV beam in the field of the circularly polarized IR laser. For particular cases of two- and three-photon absorption this case was considered in Ref. [24]. We choose the coordinate system in such a way that the z axis is directed along the collinear photon beams and the x axis is directed along the XUV electric vector. The circular dichroism is revealed by reversing the helicity of the IR beam. This case is analogous to the single-photon ionization of aligned system by circularly polarized light when alignment is perpendicular to the direction of the beam [4]. Therefore, one can expect the circular dichroism in the angular distribution of photoelectrons,

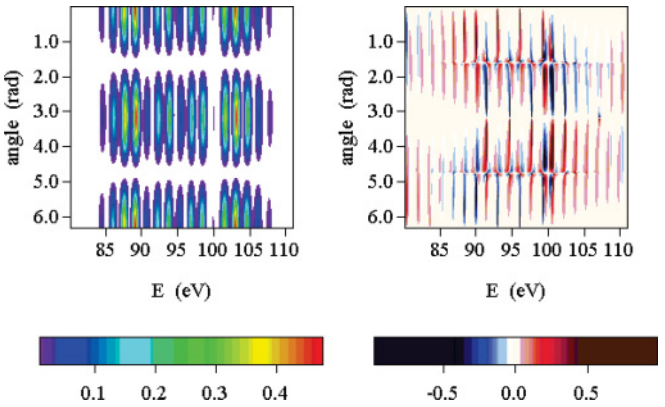

FIG. 5. (Color online) Color-scale plots of DDCS and $\mathrm{CD}^{(\mathrm{lin})}$ as functions of photoelectron energy and azimuthal emission angle φ in the plane perpendicular to the photon beams ($\theta = \pi/2$). Left panel: DDCS calculated for photoionization of He by linearly polarized XUV photons at the energy of 120 eV in the field of right-hand circularly polarized IR laser (800 nm, 2×10^{12} W/cm^2). See other parameters in text. Right panel: Circular dichroism [Eq. (15)] calculated for the same parameters.

while the integral dichroism is strictly zero. In the considered geometry, the circular dichroism appears when the projection of the electron momentum onto the plane perpendicular to the beam direction and the XUV electric vector reveal some "chirality," i.e., clockwise and anticlockwise rotations of one direction to another one are not equivalent. The chirality can be thus probed by the circularly polarized light. The dichroism is zero if photoelectrons are detected along the beam direction ($\vartheta = 0$ and π). The maximal dichroism is expected when the detector is in the plane perpendicular to the beams ($\vartheta = \pi/2$). However, the dichroism turns to zero when the photoelectrons are detected at the azimuthal angles $\varphi = n\pi/2$ when both clockwise and anticlockwise rotations are equivalent; thus, there is no chirality in experimental conditions.

As an example, we have calculated the He two-color photoionization for electron emission in the plane perpendicular to the beams (xy plane, $\vartheta = \pi/2$). The parameters of the beams are the same as in the previous section, but the intensity of the IR laser is assumed to be 2×10^{12} W/cm^2. The calculations have been done using Eqs. (13) and (14), taking into account Eq. (4). The results are shown in Figs. 5–7.

Figure 5 shows the DDCS and the CD as two-dimensional color-scale plots. The DDCS is shown in the left panel as functions of photoelectron energy and azimuthal angle φ, counted from the direction of the linear polarization of the XUV pulse. Since electrons, ionized by the XUV photons from the s shell, have a p-wave character, their angular distribution has maxima at $\varphi = 0(2\pi)$ and π and no emission at $\varphi = \pi/2$ and $3\pi/2$, which is clearly seen in the left panel of Fig. 5. The number of sidebands is obviously independent of azimuthal angle φ. The $\mathrm{CD}^{(\mathrm{lin})}$, connected with the change of helicity of the IR beam, is calculated by the formally same expression as Eq. (15). The result is shown in the right panel of Fig. 5. As expected, the CD is zero for the emission along the XUV linear polarization [$\varphi = 0(2\pi)$ and π], as well as for $\varphi = \pi/2$ and $3\pi/2$. Most interesting is the behavior of the CD for particular sidebands. One can see that the CD

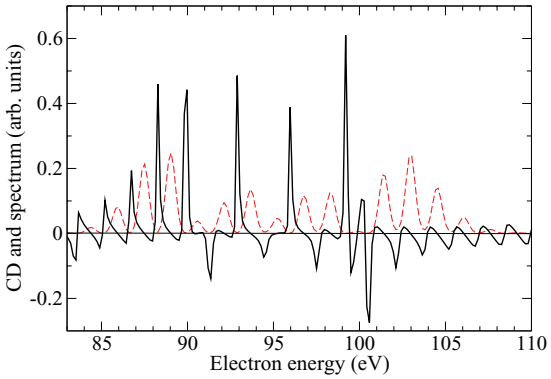

FIG. 6. (Color online) Theoretical spectrum (in arbitrary units) for laser-assisted photoionization by linearly polarized XUV light in the field of right circularly polarized IR laser (red dashed line) and $CD^{(lin)}$ in absolute units (black solid line) at emission angle $\varphi = 45^\circ$, in the plane perpendicular to the photon beams ($\theta = \pi/2$). The calculations have been done for the same parameters described in the legend of Fig. 5.

changes sign within the energy range of one sideband. It is seen more clearly in Fig. 6, where we present the spectrum and CD for the emission angle $\varphi = 45^\circ$ (a cut of the plots in Fig. 5). One can notice that within each of the spectral lines the dichroism changes sign, having zero at the maximum of the line. In general, the CD is very small within any spectral line, reaching large values only between lines where the cross section is small. Thus, in real measurements with not very good resolution, the dichroic signal will be averaged out to a small value. This is confirmed by our results for the limiting case of long pulses, obtained in the Appendix, where it is shown that the CD for an individual sideband is zero. In Fig. 7 the angular distribution for two spectral lines is shown. The CD is antisymmetrical with respect to $\varphi = \pi$. As we have mentioned, the CD is zero near $\varphi = n\pi/2$. The character of the angular distributions is similar for all lines. Similar angular distributions have been obtained for two-photon absorption in Ref. [24]. By dot-dashed lines in Fig. 7 we show the CD, calculated with the cross sections convoluted with the Gaussian curve imitating the typical overall apparatus energy resolution of 0.8 eV. The resulting CD becomes small (less then 5%). We note that our result is consistent with the results of Ref. [24], where it was shown that CD for the case of linearly polarized XUV pulse tends to zero at large electron energy.

C. Linear dichroism with linearly polarized XUV beam

When both XUV and IR beams are linearly polarized, one can consider the difference in the yield of photoelectrons for two mutually perpendicular directions of the linear polarization of one of the beams. In the case of single-photon absorption, the difference in photoelectron yields for parallel and perpendicular polarizations of the two beams is called linear dichroism (LD) or linear alignment dichroism [4]. Here we consider LD in the two-color multiphoton ionization. We assume that the direction of the linear polarization of the XUV beam, propagating along the z axis, is fixed along the x axis. The linear polarization of the collinear IR beam can be rotated and the LD can be studied. The angular distribution of photoelectrons in this case is symmetrical with respect to the plane perpendicular to the beams (xy plane). Usually the angular distribution of photoelectrons and LD are measured in this plane.

The calculated DDCSs and LD as functions of photoelectron energy and the azimuthal emission angle φ are shown in Fig. 8 for the two-color photoionization of He ($1s$) for the same parameters of pulses as in previous sections. It is assumed that photoelectrons are registered in the xy plane perpendicular to the photon beams. The left panel shows the results when linear polarizations of the XUV and IR beams are parallel and directed along the x axis. The system of sidebands is clearly seen with maximum number of sidebands at $\varphi = 0$ and π. The number of sidebands quickly diminishes with increase of angle from 0 to $\pi/2$. Because of the p-wave character of photoemission by XUV photons, the photoelectron intensity at $\varphi = \pi/2$ is zero. The central panel shows the calculated DDCS for the case of perpendicular polarizations of the beams. When the emission angle is zero or π the intensity of the photoline produced by the XUV photons is maximal. However, there

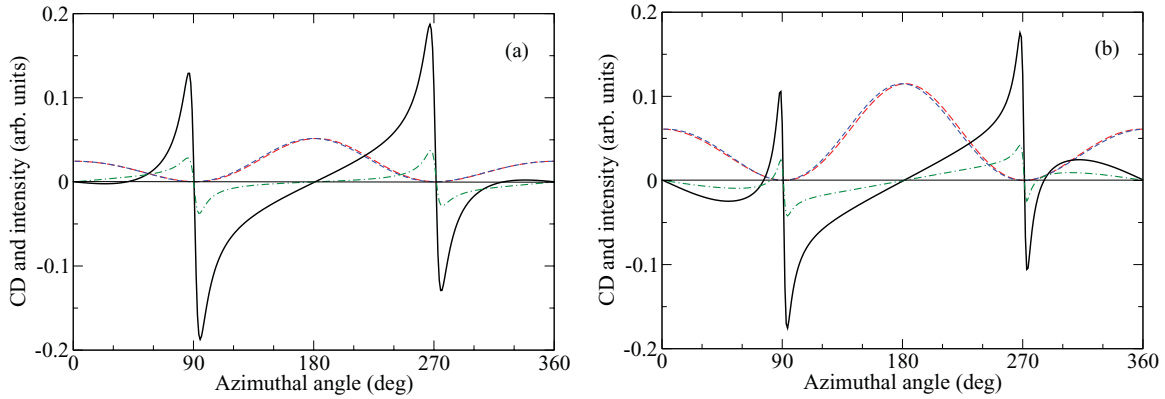

FIG. 7. (Color online) Calculated angular distributions of photoelectrons (in arbitrary units) generated by linearly polarized XUV light in the field of right (red long-dashed line) and left (blue short-dashed line) circularly polarized IR light; the angular distribution of $CD^{(lin)}$ in absolute units is shown by black solid line: (a) for the central line at the energy of 95.4 eV and (b) for the first sideband at the energy of 97.0 eV. The observation plane is perpendicular to the photon beams ($\theta = \pi/2$). All parameters are the same as described in the legend of Fig. 5. The dot-dashed lines show the averaged CD (see text).

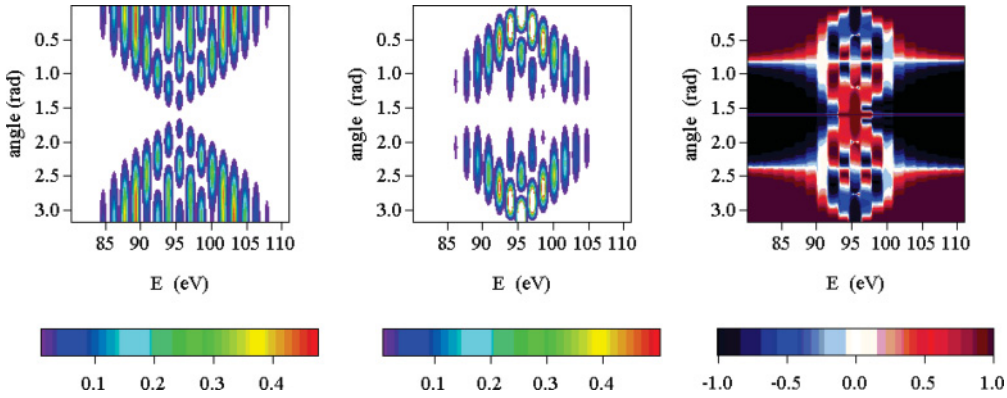

FIG. 8. (Color online) Color-scale plots of DDCSs and LD as functions of photoelectron energy and azimuthal angle φ in the plane perpendicular to the beams ($\theta = \pi/2$). Left panel: DDCS calculated for photoionization of He by linearly polarized XUV photons at the energy of 120 eV in the field of linearly polarized IR laser for parallel polarizations of the beams. Central panel: the same for perpendicular polarizations of the beams. Right panel: LD [Eq. (21)]. All parameters are the same as described in the legend of Fig. 5

are no sidebands because the IR field is now perpendicular to the electron velocity. The maximum number of sidebands could be expected at emission angle $\varphi = \pi/2$. However, no photoelectrons are emitted at this angle by the XUV photons.

The LD is defined as

$$\mathrm{LD} = \frac{|\mathcal{A}_{\vec{k}}^{\parallel}|^2 - |\mathcal{A}_{\vec{k}}^{\perp}|^2}{|\mathcal{A}_{\vec{k}}^{\parallel}|^2 + |\mathcal{A}_{\vec{k}}^{\perp}|^2}, \tag{21}$$

where $\mathcal{A}_{\vec{k}}^{\parallel}$ and $\mathcal{A}_{\vec{k}}^{\perp}$ are amplitudes of photoionization for parallel and perpendicular polarizations of ionizing beams, respectively. The calculated LD for He multiphoton ionization is presented in the right panel as a two-dimensional color-scale plot. Here red (medium gray) color indicates positive dichroism while blue (dark grey) color indicates negative dichroism. The LD is practically constant within every particular sideband, sharply changing its sign for the neighboring sidebands at least for the low-order sidebands. Also within one sideband the LD shows quick variation with angle and change of sign several times. At emission angles 0 and π the LD =1 for all sidebands except the central line. This is clear from definition Eq. (21) and the fact that at these angles the intensity of sidebands in perpendicular case is zero. At the emission angle $\varphi = \pi/4$ ($3\pi/4$), the LD = 0 since the cross sections for parallel and perpendicular polarizations are equal. At $\varphi = \pi/2$, the LD is not defined since both cross sections are zero. (The horizontal lines seen in this figure at $\varphi = \pi/2$ are artifacts.)

In more detail, the spectra and LD are shown in Fig. 9 for a particular emission angle $\varphi = 40^\circ$. The stepwise character of the LD and the alternating signs for low-order sidebands is clearly seen. For high-order sidebands the sign of LD is positive. Note that the absolute value of LD is rather high in this case. Figure 10 displays the angular distributions of photoelectrons for two neighboring sidebands and corresponding LD. The general character of the LD as function of emission angle is similar to the cases of CD: quick variation with angle and change of sign several times. Remember, in the small energy interval around $\varphi = \pi/2$, the LD is not defined due to extremely small cross sections. In the Appendix we have derived an expression, Eq. (A25), for the LD for long XUV and IR pulses, which can serve as approximate expression for quick and easy estimation of the expected effect. For a particular geometry considered here ($\vartheta = \pi/2$), one gets the dependence of LD on the emission angle φ for the mth sideband:

$$\mathrm{LD}_m = \frac{|J_m(\bar{q}_{\parallel})|^2 - |J_m(\bar{q}_{\perp})|^2}{|J_m(\bar{q}_{\parallel})|^2 + |J_m(\bar{q}_{\perp})|^2}, \tag{22}$$

where $\bar{q}_{\parallel} = \frac{A_L k}{\omega_L}\cos\varphi$ and $\bar{q}_{\perp} = \frac{A_L k}{\omega_L}\sin\varphi$. From this expression one can easily obtain all the peculiarities mentioned above. For example, if $\varphi = 0$ (an electron is emitted along the XUV polarization), $\bar{q}_{\perp} = 0$ and all Bessel functions $J_m(q_{\perp})$ except $J_0(q_{\perp})$ turn to zero; thus, LD= 1 when $m \neq 0$; if $\varphi = \pi/4$, then $\bar{q}_{\perp} = \bar{q}_{\parallel}$ and LD =0 for all sidebands, etc.

Similar to the case of two circularly polarized beams, also for the linearly polarized IR and XUV beams, the angle-integrated cross section reveals LD. The calculated angle-integrated cross sections and the LD are shown in Fig. 11(a) for the same conditions as above. The angle-integrated LD is quite large, being of the order of unity. Note that at the considered IR

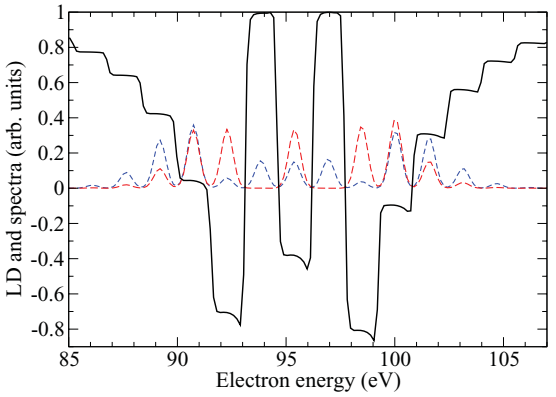

FIG. 9. (Color online) Theoretical spectrum (in arbitrary units) for laser-assisted photoionization by linearly polarized XUV pulse in the field of linearly polarized IR laser for parallel (blue short-dashed line) and perpendicular (red long-dashed line) polarizations, and LD in absolute units (black solid line) at the emission angle $\varphi = 40^\circ$ in the plane perpendicular to the beams ($\theta = \pi/2$). The parameters of the beams are the same as described in the legend of Fig. 5.

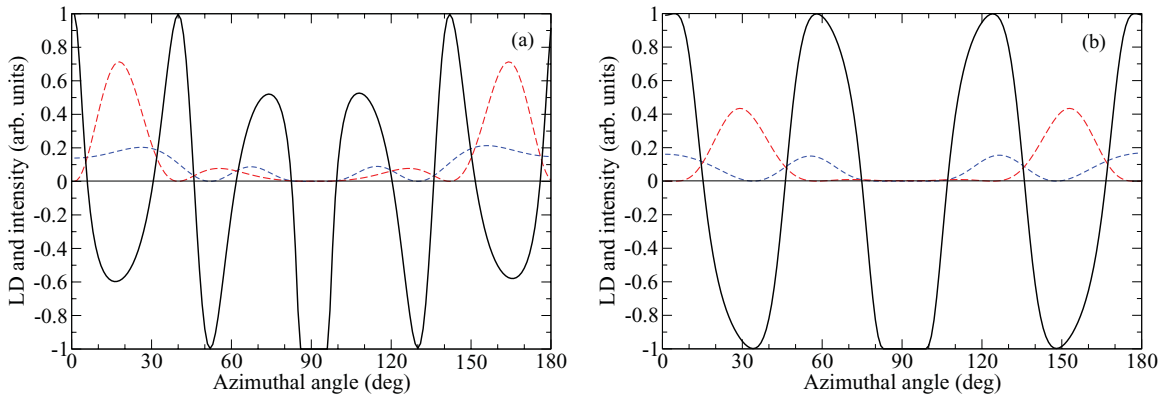

FIG. 10. (Color online) Calculated angular distributions of photoelectrons (in arbitrary units) generated by linearly polarized XUV and IR pulses with parallel (blue short-dashed line) and perpendicular (red long-dashed line) polarizations and angular distribution of LD in absolute units (black solid line): (a) for the first sideband at the energy of 97.0 eV and (b) for the second sideband at the energy of 98.5 eV. All other parameters are the same as described in the legend of Fig. 5.

laser flux, the dichroism for the low-order sidebands is negative while for the higher-order sidebands it is positive. Negative LD means that the intensity of the sideband for the perpendicular polarizations is larger than for the parallel ones. In the only published experiment [21] where the dependence of intensity of the first sideband on the angle between polarizations was measured, the intensity was larger for the parallel rather than for perpendicular polarizations. However, in that experiment, the IR pulse was rather weak, 8×10^{10} W/cm^2. In Fig. 11(b) we show the results of the LD calculations for this intensity. Here even for the first sideband the dichroism is positive, which is consistent with the experimental data and the calculations within the soft-photon approximation [21].

IV. SUMMARY AND CONCLUDING REMARKS

We have analyzed different types of dichroism in short-pulse two-color XUV + IR multiphoton ionization of unpolarized atoms when in the photoelectron spectrum a well-developed sideband structure appears. In particular, three cases have been considered: (a) CD$^{(\mathrm{circ})}$ when both IR and XUV pulses are circularly polarized, (b) CD$^{(\mathrm{lin})}$ when the IR pulse is circularly polarized while the XUV pulse is linearly polarized, and (c) LD when both pulses are linearly polarized. The calculations have been done within the SFA approach for the realistic pulse durations and optical laser intensities similar to those used in experiments at FELs such as FLASH and LCLS. Thus, one can use the results for planning future experiments. The numerical evaluations are confirmed by the analytical results obtained for comparatively long XUV and IR pulses. In cases (a) and (c) the dichroic effect in the angular distribution of photoelectrons is quite substantial and can be measured with the modern experimental facilities. In case (b) the CD is small and its measurements might be prohibitively difficult at least for large photoelectron energies. In all cases the dichroism is shown to variate strongly from one sideband to another. It also changes considerably with the emission angle. The study of the circular and linear dichroism gives deeper insight into the dynamics of the interaction of short intense pulses with atoms and molecules, since the dichroism is sensitive both to the values and to the phases of the matrix elements involved. Besides, such measurements can be used

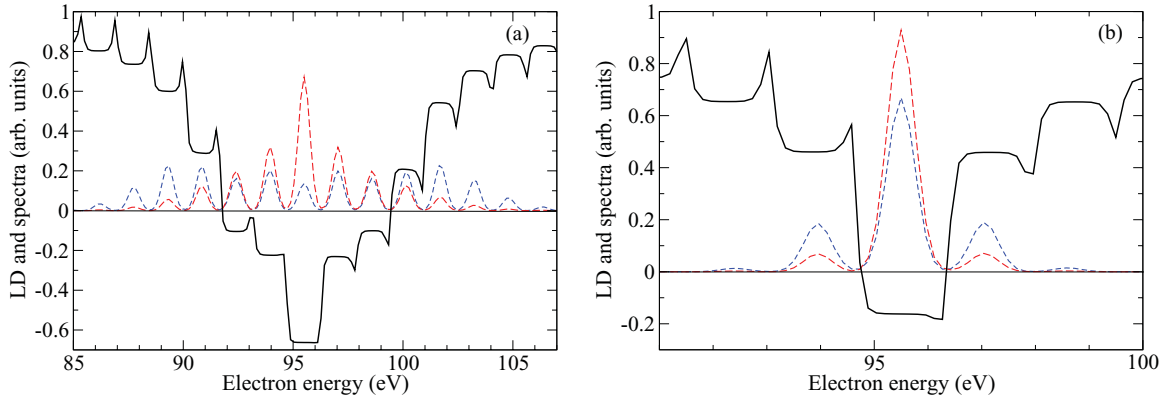

FIG. 11. (Color online) Angle-integrated yield of photoelectrons (in arbitrary units) generated by linearly polarized XUV and IR lights with parallel (blue short-dashed line) and perpendicular (red long-dashed line) polarizations and the LD in absolute units (black solid line): (a) for the IR field of 2×10^{12} W/cm^2 and (b) for the IR field of 8×10^{10} W/cm^2. All other parameters are the same as described in the legend of Fig. 5.

for characterization of the FEL photon beams. Particularly, the measurements of the CD with circularly polarized XUV beam can be of certain interest, since they can be used for measuring and/or monitoring the circular polarization of the XUV beam in the energy range where there is no other effective methods [26].

ACKNOWLEDGMENTS

The authors are grateful to M. Meyer for numerous useful discussions and for critical reading of the manuscript and to K. Ueda for stimulating discussions. N.M.K. is grateful to Donostia International Physics Center (DIPC) for hospitality and for financial support.

APPENDIX

Let us derive Eqs. (16) and (18) for the case of a very long IR pulse. Suppose that the IR pulse is circularly polarized, then the pulse electric field may be presented as

$$\mathcal{E}_L(t) = g(\alpha t)\frac{\bar{\mathcal{E}}_L}{\sqrt{2}}\left[\hat{x}\cos(\omega_L t) \pm \hat{y}\sin(\omega_L t)\right], \qquad \text{(A1)}$$

where $\bar{\mathcal{E}}_L$ is the field amplitude and upper (lower) sign corresponds to right (left) circularly polarized IR field. The corresponding vector potential is

$$A_L(t) = g(\alpha t)A_L\left[\hat{x}\sin(\omega_L t) \mp \hat{y}\cos(\omega_L t)\right] \qquad \text{(A2)}$$

with $A_L = -\bar{\mathcal{E}}_L/\sqrt{2}\omega_L$. Here and in Eq. (A1) we have introduced an auxiliary function $g(x)$, which is smooth, equal to unity at small x, and tends to zero limit at large $|x|$. It allows us to calculate the integral Eq. (6) when the upper limit $T \to \infty$ and $\alpha \to 0$. In the following we assume that $k \gg A_L$ and ignore the quadratic term A_L^2 in Eq. (14). In this approximation, taking into account that $k_x = k\sin\vartheta\cos\varphi$ and $k_y = k\sin\vartheta\sin\varphi$, the Volkov phase can be presented as

$$\Phi(\vec{k},t) = \frac{k^2}{2}t + \frac{kA_L}{\omega_L}\sin\vartheta\cos(\varphi \mp \omega_L t). \qquad \text{(A3)}$$

Substituting this expression into Eq. (14) and using the Jacobi-Anger expansion

$$\exp(i\kappa\cos\alpha) = \sum_{m=-\infty}^{+\infty} i^m \exp(im\alpha)J_m(\kappa), \qquad \text{(A4)}$$

where $J_m(\kappa)$ is the Bessel function, one obtains

$$\mathcal{F}(\vec{k}) = -\sum_{m=-\infty}^{+\infty}\int_{-\infty}^{\infty} dt\,\tilde{\mathcal{E}}_X(t)Y_{1,1}(\vartheta_0,\varphi_0)i^m\exp(im\varphi) \times \exp(\mp im\omega_L t)J_m(q)\exp\left[i(E_b + \frac{k^2}{2} - \omega_X)t\right], \qquad \text{(A5)}$$

where $q = kA_L\sin\vartheta/\omega_L$ and we assumed that the XUV pulse is right circularly polarized. The spherical harmonic $Y_{1,1}(\vartheta_0,\varphi_0)$ can be expressed in terms of angles ϑ,φ using Eqs. (9) and (10) as follows:

$$\begin{aligned} Y_{1,1}(\vartheta_0,\varphi_0) &\equiv -\sqrt{\frac{3}{8\pi}}\sin\vartheta_0\exp(i\varphi_0) \\ &\approx -\sqrt{\frac{3}{8\pi}}\left[\sin\vartheta\exp(i\varphi) \pm i\frac{A_L}{k}\exp(\pm i\omega_L t)\right. \\ &\quad \left. + \frac{A_L}{k}\sin^2\vartheta\exp(i\varphi)\sin(\omega_L t \mp \varphi)\right]. \end{aligned} \qquad \text{(A6)}$$

Here upper (lower) sign corresponds to the right (left) circular polarization of the IR field, and we have kept only linear term in A_L/k, which is considered to be small $A_L/k \ll 1$.

Substituting this expression for the right circular polarization of the IR pulse (upper signs) into Eq. (A5) one obtains the factor $\mathcal{F}_R(\vec{k})$

$$\begin{aligned} \mathcal{F}_R(\vec{k}) = \sqrt{\frac{3}{8\pi}}\sum_{m=-\infty}^{+\infty} i^m\exp(-im\varphi)J_m(q) \\ \times\left[\sin\vartheta\exp(i\varphi)\tilde{\mathcal{E}}_X^{(m)} + i\frac{A_L}{2k}(2-\sin^2\vartheta)\,\tilde{\mathcal{E}}_X^{(m+1)}\right. \\ \left. + i\frac{A_L}{2k}\sin^2\vartheta\;\exp(2i\varphi)\tilde{\mathcal{E}}_X^{(m-1)}\right], \end{aligned} \qquad \text{(A7)}$$

where the following notation is introduced:

$$\tilde{\mathcal{E}}_X^{(m)} = \int_{-\infty}^{\infty} dt\tilde{\mathcal{E}}_X(t)\exp\left[i\left(E_b - \omega_X + \frac{k^2}{2} + im\omega_L\right)t\right]. \qquad \text{(A8)}$$

This expression can be rewritten by rearranging the terms in the sums as

$$\begin{aligned} \mathcal{F}_R(\vec{k}) &= \sqrt{\frac{3}{8\pi}}\sum_{n=-\infty}^{+\infty}\tilde{\mathcal{E}}_X^{(n)}i^n\exp[i(1-n)\varphi] \\ &\quad\times\left[\sin\vartheta\,J_n(q) + \frac{A_L}{2k}(2-\sin^2\vartheta)\;J_{n-1}(q)\right. \\ &\quad\left. - \frac{A_L}{2k}\sin^2\vartheta\;J_{n+1}(q)\right] \\ &= \sqrt{\frac{3}{8\pi}}\sum_{n=-\infty}^{+\infty}\tilde{\mathcal{E}}_X^{(n)}i^n\exp[i(1-n)\varphi] \\ &\quad\times\left[\sin\vartheta\left(1 - \frac{n\omega_L}{k^2}\right)J_n(q) + \frac{A_L}{k}J_{n-1}(q)\right]. \end{aligned} \qquad \text{(A9)}$$

Similarly, for the case of left circular polarization of the IR pulse one can obtain the factor $\mathcal{F}_L(\vec{k})$ by substituting Eq. (A6) with lower signs into Eq. (A5):

$$\begin{aligned} \mathcal{F}_L(\vec{k}) = \sqrt{\frac{3}{8\pi}}\sum_{n=-\infty}^{+\infty}\tilde{\mathcal{E}}_X^{(n)}i^n\exp[i(n+1)\varphi] \\ \times\left[\sin\vartheta\left(1 - \frac{n\omega_L}{k^2}\right)J_n(q) + \frac{A_L}{k}J_{n+1}(q)\right]. \end{aligned} \qquad \text{(A10)}$$

If the XUV pulse is left circularly polarized [Eq. (A5) contains $Y_{1-1}(\vartheta_0,\varphi_0)$], the amplitudes for right and left

circularly polarized IR radiation look, respectively, as

$$\mathcal{F}_R(\vec{k}) = \sqrt{\frac{3}{8\pi}} \sum_{n=-\infty}^{+\infty} \tilde{\mathcal{E}}_X^{(n)} i^n \exp[-i(n+1)\varphi] \times \left[\sin\vartheta \left(1 - \frac{n\omega_L}{k^2}\right) J_n(q) + \frac{A_L}{k} J_{n+1}(q) \right], \quad \text{(A11)}$$

and

$$\mathcal{F}_L(\vec{k}) = \sqrt{\frac{3}{8\pi}} \sum_{n=-\infty}^{+\infty} \tilde{\mathcal{E}}_X^{(n)} i^n \exp[i(n-1)\varphi] \times \left[\sin\vartheta \left(1 - \frac{n\omega_L}{k^2}\right) J_n(q) + \frac{A_L}{k} J_{n-1}(q) \right]. \quad \text{(A12)}$$

If the XUV pulse is sufficiently long, covering many oscillations of the IR field, then the function $\tilde{\mathcal{E}}_X^{(n)}$ is close to the δ function [Eq. (19)], and for each of the sidebands (for each n) one can ignore the contributions from all other terms and interference between the sidebands. Then the intensity of the sideband, I_n, is proportional to the square of the nth term in the sum $I_n \sim |\mathcal{F}_{R(L)}^{(n)}|^2$ for right (R) and left (L) circularly polarized IR fields.

The CD is determined by the difference of the cross sections for the right and left circularly polarized light, which is proportional (for a particular n) to $|\mathcal{F}_R^{(n)}(\vec{k})|^2 - |\mathcal{F}_L^{(n)}(\vec{k})|^2$. Using Eqs. (A9) and (A10), one can obtain

$$\left|\mathcal{F}_R^{(n)}(\vec{k})\right|^2 - \left|\mathcal{F}_L^{(n)}(\vec{k})\right|^2 = \frac{3}{8\pi} \left|\tilde{\mathcal{E}}_X^{(n)}\right|^2 4 \frac{A_L}{k} J_n(q) \frac{dJ_n(q)}{dq} \times \left[\sin\vartheta \left(1 - \frac{n\omega_L}{k^2}\right) + \frac{n\omega_L}{k^2 \sin\vartheta} \right]. \quad \text{(A13)}$$

For relative dichroism one needs to calculate also the sum of the cross sections which is proportional to

$$\left|\mathcal{F}_R^{(n)}(\vec{k})\right|^2 + \left|\mathcal{F}_L^{(n)}(\vec{k})\right|^2 = \frac{3}{8\pi} \left|\tilde{\mathcal{E}}_X^{(n)}\right|^2 2 \left\{ J_n^2(q) \left[\sin\vartheta \left(1 - \frac{n\omega_L}{k^2}\right) + \frac{n\omega_L}{k^2 \sin\vartheta} \right]^2 + \frac{A_L^2}{k^2} \left[\frac{dJ_n(q)}{dq} \right]^2 \right\}. \quad \text{(A14)}$$

The ratio of Eqs. (A13) and (A14) gives relative CD for the nth sideband:

$$\mathrm{CD}_n^{(\mathrm{circ})} \equiv \frac{\left|\mathcal{F}_R^{(n)}(\vec{k})\right|^2 - \left|\mathcal{F}_L^{(n)}(\vec{k})\right|^2}{\left|\mathcal{F}_R^{(n)}(\vec{k})\right|^2 + \left|\mathcal{F}_L^{(n)}(\vec{k})\right|^2} = 2 \frac{A_L}{k} J_n(q) \frac{dJ_n(q)}{dq} \left[\sin\vartheta \left(1 - \frac{n\omega_L}{k^2}\right) + \frac{n\omega_L}{k^2 \sin\vartheta} \right] \times \left\{ J_n^2(q) \left[\sin\vartheta \left(1 - \frac{n\omega_L}{k^2}\right) + \frac{n\omega_L}{k^2 \sin\vartheta} \right]^2 + \frac{A_L^2}{k^2} \left[\frac{dJ_n(q)}{dq} \right]^2 \right\}^{-1}. \quad \text{(A15)}$$

If the XUV beam is linearly polarized, the corresponding amplitude can be obtained by summing amplitudes for right and left circularly polarized XUV beams. Thus, for the right circularly polarized IR radiation one should sum Eqs. (A9) and (A11), which gives

$$\mathcal{F}_R(\vec{k}) = \sqrt{\frac{3}{8\pi}} \sum_{n=-\infty}^{+\infty} \tilde{\mathcal{E}}_X^{(n)} i^n \exp(-in\varphi) \times \left\{ 2\cos\varphi \sin\vartheta \left(1 - \frac{n\omega_L}{k^2}\right) J_n(q) + \frac{A_L}{k} [e^{i\varphi} J_{n-1}(q) + e^{-i\varphi} J_{n+1}(q)] \right\}. \quad \text{(A16)}$$

For the left circularly polarized IR radiation one gets by summing Eqs. (A10) and (A12):

$$\mathcal{F}_L(\vec{k}) = \sqrt{\frac{3}{8\pi}} \sum_{n=-\infty}^{+\infty} \tilde{\mathcal{E}}_X^{(n)} i^n \exp(in\varphi) \times \left\{ 2\cos\varphi \sin\vartheta \left(1 - \frac{n\omega_L}{k^2}\right) J_n(q) + \frac{A_L}{k} [e^{i\varphi} J_{n+1}(q) + e^{-i\varphi} J_{n-1}(q)] \right\}. \quad \text{(A17)}$$

Comparing Eqs. (A16) and (A17), we see that expressions in square brackets are complex conjugate. Therefore, for each particular sideband (individual n) the cross sections, calculated within our approximation for infinitely long IR pulse, are equal for left and right circularly polarized light and CD is strictly zero. Nonzero dichroism for finite pulses is discussed in Sec. III B.

Now we consider the case when both beams are linearly polarized. As above, we consider collinear beams propagating along the z axis. We choose the x axis along the polarization vector of XUV pulse and suppose that the IR polarization is directed at the angle χ relative to the x axis. In this case, the vector potential of the IR field may be presented as

$$A_L(t) = g(\alpha t) A_L \sin(\omega_L t)[\hat{x}\cos\chi + \hat{y}\sin\chi]. \quad \text{(A18)}$$

The Volkov phase in this case is

$$\Phi(\vec{k},t) = \frac{k^2}{2}t + \frac{kA_L}{\omega_L} \sin\vartheta \cos(\varphi - \chi)\cos(\omega_L t). \quad \text{(A19)}$$

Expanding the amplitude in terms of Bessel functions, we obtain

$$\mathcal{F}(\vec{k}) = \sum_{m=-\infty}^{+\infty} \int_{-\infty}^{\infty} dt\, \tilde{\mathcal{E}}_X(t) [\mathrm{Re}Y_{1,1}(\vartheta_0,\varphi_0)] i^m \exp(im\varphi) \times \exp(im\omega_L t) J_m(\bar{q}) \exp\left[i\left(E_b + \frac{k^2}{2} - \omega_X\right)t \right], \quad \text{(A20)}$$

where $\bar{q} = \frac{A_L k}{\omega_L} \sin\vartheta\cos(\varphi - \chi)$. The operator $-\mathrm{Re}Y_{1,1}(\vartheta_0,\varphi_0)$ corresponds to the XUV light polarized along x axis. In analogy with the previous case of circular polarized light, we obtain the following expression for this operator in terms of emission angles ϑ and φ:

$$\mathrm{Re}Y_{1,1}(\vartheta_0,\varphi_0) \equiv -\sqrt{\frac{3}{8\pi}} \sin\vartheta_0 \cos\varphi_0 \approx -\sqrt{\frac{3}{8\pi}} \left\{ \sin\vartheta\cos\varphi - \frac{A_L}{k} [\cos\chi - \sin^2\vartheta \times \cos\varphi\cos(\varphi - \chi)] \sin(\omega_L t) \right\}. \quad \text{(A21)}$$

Substituting this expression in Eq. (A20) we get

$$\mathcal{F}(\vec{k}) = \sum_{m=-\infty}^{+\infty} \mathcal{E}_X^{(m)} i^m \exp(im\varphi) J_m(\bar{q}) \times \left[\sin\vartheta\cos\varphi + \frac{A_L m}{k\bar{q}} f(\vartheta,\varphi,\chi)\right], \quad \text{(A22)}$$

where $f(\vartheta,\varphi,\chi) = \cos\chi - \sin^2\vartheta\cos\varphi\cos(\varphi-\chi)$. For not very large m we can ignore the second term in the square brackets due to the small value of ω_L/k^2 and obtain

$$\mathcal{F}(\vec{k}) = \sum_{m=-\infty}^{+\infty} \mathcal{E}_X^{(m)} i^m \exp(im\varphi) J_m(\bar{q}) \sin\vartheta\cos\varphi. \quad \text{(A23)}$$

Thus, for the mth sideband the angular distribution and the dependence on the angle χ between polarizations is determined by the expression

$$\sigma^{(m)}(\vec{k}) \sim |J_m(\bar{q})|^2 \sin^2\vartheta\cos^2\varphi. \quad \text{(A24)}$$

Using this expression one can calculate the LD for a particular sideband. Since the LD, defined by Eq. (21), is determined by the difference of the cross sections for parallel ($\chi = 0$) and perpendicular ($\chi = \pi/2$) orientation of the photon polarizations, one obtains for the mth sideband and for $\vartheta \neq 0$

$$\mathrm{LD}_m = \frac{|J_m(\bar{q}_\parallel)|^2 - |J_m(\bar{q}_\perp)|^2}{|J_m(\bar{q}_\parallel)|^2 + |J_m(\bar{q}_\perp)|^2}, \quad \text{(A25)}$$

where $\bar{q}_\parallel = \frac{A_L k}{\omega_L}\sin\vartheta\cos\varphi$ and $\bar{q}_\perp = \frac{A_L k}{\omega_L}\sin\vartheta\sin\varphi$.

[1] G. Schönhense and J. Hormes, in *VUV and Soft X-Ray Photoionization*, edited by U. Becker and D. A. Shirley (Plenum Press, New York, 1996), p. 607.
[2] K. Starke, *Magnetic Dichroism in Core-Level Photoemission* (Springer, Berlin, 2000).
[3] N. M. Kabachnik, S. Fritzsche, A. N. Grum-Grzhimailo, M. Meyer, and K. Ueda, Phys. Rep. **451**, 155 (2007).
[4] N. A. Cherepkov, V. V. Kuznetsov, and V. A. Verbitskii, J. Phys. B **28**, 1221 (1995).
[5] A. N. Grum-Grzhimailo and M. Meyer, Eur. Phys. J. Special Topics **169**, 43 (2009).
[6] A. Verweyen, A. N. Grum-Grzhimailo, and N. M. Kabachnik, Phys. Rev. A **60**, 2076 (1999).
[7] G. Prümper, O. Geßner, B. Zimmermann, J. Viefhaus, R. Hentges, H. Kleinpoppen, and U. Becker, J. Phys. B **34**, 2707 (2001).
[8] O. Plotzke, G. Prümper, B. Zimmermann, U. Becker, and H. Kleinpoppen, Phys. Rev. Lett. **77**, 2642 (1996).
[9] Ph. Wernet, A. Verweyen, J. Schulz, B. Sonntag, K. Godehusen, R. Müller, P. Zimmermann, and M. Martins, J. Phys. B **35**, 3887 (2002).
[10] Ph. Wernet, J. Schulz, B. Sonntag, K. Godehusen, P. Zimmermann, A. N. Grum-Grzhimailo, N. M. Kabachnik, and M. Martins, Phys. Rev. A **64**, 042707 (2001).
[11] A. N. Grum-Grzhimailo, E. V. Gryzlova, D. Cubaynes, E. Heinecke, M. Yalçinkaya, P. Zimmermann, and M. Meyer, J. Phys. B **42**, 171002 (2009).
[12] J. Schulz, Ph. Wernet, M. Martins, B. Sonntag, R. Müller, K. Godehusen, and P. Zimmermann, Phys. Rev. A **67**, 012502 (2003).
[13] J. Niskanen, S. Urpelainen, K. Jänkälä, J. Schulz, S. Heinäsmäki, S. Fritzsche, N. M. Kabachnik, S. Aksela, and H. Aksela, Phys. Rev. A **81**, 013406 (2010).
[14] H. Klar and H. Kleinpoppen, J. Phys. B **15**, 933 (1982).
[15] F. J. Wuilleumier and M. Meyer, J. Phys. B **39**, R425 (2006).
[16] M. Meyer, J. T. Costello, S. Düsterer, W. B. Li, and P. Radcliffe, J. Phys. B **42**, 194006 (2010).
[17] T. E. Glover, R. W. Schoenlein, A. H. Chin, and C. V. Shank, Phys. Rev. Lett. **76**, 2468 (1996).
[18] E. S. Toma, H. G. Muller, P. M. Paul, P. Breger, M. Cheret, P. Agostini, C. Le Blanc, G. Mullot, and G. Cheriaux, Phys. Rev. A **62**, 061801(R) (2000).
[19] P. O'Keeffe, R. Lopez-Martens, J. Mauritsson, A. Johansson, A. L'Huillier, V. Véniard, R. Taïeb, A. Maquet, and M. Meyer, Phys. Rev. A **69**, 051401(R) (2004).
[20] M. Meyer *et al.*, Phys. Rev. A **74**, 011401(R) (2006).
[21] M. Meyer *et al.*, Phys. Rev. Lett. **101**, 193002 (2008).
[22] S. Düsterer *et al.*, New J. Phys. **13**, 093024 (2011).
[23] N. L. Manakov, A. Maquet, S. I. Marmo, V. Veniard, and G. Ferrante, J. Phys. B **32**, 3747 (1999).
[24] R. Taïeb, V. Véniard, A. Maquet, N. L. Manakov, and S. I. Marmo, Phys. Rev. A **62**, 013402 (2000).
[25] P. Lambropoulos, Phys. Rev. Lett. **29**, 453 (1972).
[26] A. K. Kazansky, A. V. Grigorieva, and N. M. Kabachnik, Phys. Rev. Lett. **107**, 253002 (2011).
[27] A. K. Kazansky, I. P. Sazhina, and N. M. Kabachnik, Phys. Rev. A **82**, 033420 (2010).
[28] A. K. Kazansky and N. M. Kabachnik, J. Phys. B **39**, 5173 (2006).
[29] A. K. Kazansky and N. M. Kabachnik, J. Phys. B **40**, 2163 (2007).
[30] A. K. Kazansky and N. M. Kabachnik, J. Phys. B **40**, 3413 (2007).
[31] M. Lewenstein, P. Balcou, M. Y. Ivanov, A. L'Huillier, and P. B. Corkum, Phys. Rev. A **49**, 2117 (1994).
[32] F. Quéré, Y. Mairesse, and J. Itatani, J. Mod. Opt. **52**, 339 (2005).
[33] L. V. Keldysh, Sov. Phys. JETP **20**, 1307 (1965).
[34] L. D. Landau and E. M. Lifshitz, *Quantum Mechanics: Nonrelativistic Theory* (Pergamon, New York, 1979).
[35] D. B. Wolkow, Z. Phys. **94**, 250 (1935).
[36] I. I. Sobelman *Introduction to the Theory of Atomic Spectra* (Pergamon, Oxford, 1972).
[37] N. M. Kabachnik, J. Electron Spectrosc. Relat. Phenom. **79**, 269 (1996).
[38] E. Allaria, C. Callegari, D. Cocco, W. M. Fawley, M. Kiskinova, C. Masciovecchio, and F. Parmigiani, New J. Phys. **12**, 075002 (2010).